Efficient Beam-Type Structural Modeling of Rotor Blades

Couturier, Philippe; Krenk, Steen

Published in:
Proceedings of the EWEA Annual Event and Exhibition 2015

Publication date:
2015

Document Version
Peer reviewed version

Efficient Beam-Type Structural Modeling of Rotor Blades

Philippe J. Couturier* and Steen Krenk†
Technical University of Denmark, DK-2800, Kongens Lyngby, Denmark

Abstract

The present paper presents two recently developed numerical formulations which enable accurate representation of the static and dynamic behaviour of wind turbine rotor blades using little modeling and computational effort. The first development consists of an intuitive method to extract fully coupled six by six cross-section stiffness matrices with limited meshing effort. Secondly, an equilibrium based beam element accepting directly the stiffness matrices and accounting for large variations in geometry and material along the blade is presented. The novel design tools are illustrated by application to a composite section with bend-twist coupling and a real wind turbine blade.

1 Introduction

Wind turbine rotors are becoming increasingly slender with the introduction of larger rotors, inviting global beam-type analysis which puts focus on underlying beam theory and general cross-sectional stiffness properties. The blade modeling approach must provide accurate predictions of the blade behavior, e.g. bend-twist response while being able to easily accommodate geometry and material updates from previous designs.

This paper presents a developed methodology to facilitate the design of wind turbine blades using anisotropic materials and complex geometry to generate desired displacement characteristics. The work was done as part of a collaborative project between the Technical University of Denmark and Siemens Wind Power A/S. In the first part of the project a formulation was developed for analysis of the properties of general cross-sections with arbitrary geometry and material distribution [1]. The work was later extended by an efficient finite element modelling approach for thin and thick-walled sections which substantially reduced the meshing effort by discretizing the walls of the section using a single layer of displacement based elements with the layers represents within the elements [2]. The last part of the project aimed at showing how these general properties enter an efficient equilibrium based beam element which accounts for geometry and material variations along the blade span based on Krenk [3]. The beam element has been incorporated into an aeroelastic program at Siemens Wind Power A/S.

2 Approach

The basic process of structural modeling routinely used for slender structures, like wind turbine blades, to obtain fast and accurate predictions of the natural frequencies, deflections, and the overall dynamic behaviour is shown in Fig. 1. The goal of the process is to construct a reduced model of the 3D composite structure using beam elements. For an accurate representation, the beam model must reproduce the elastic energy of the 3D structure. This can only be achieved if one accounts for the variations in cross-section geometry and material properties along the blade as well as the governing kinematic behaviours, e.g. deformation mode coupling, transverse shear deformation and warping.

The first step to reduce the dimensionality of a blade is to calculate the mechanical properties associated with the individual beam cross-sections. As part of the project, a formulation for cross-section analysis providing the full six by six stiffness matrix for non-homogeneous and anisotropic

*PhD Candidate, Department of Mechanical Engineering; currently Engineer, Siemens Wind Power, Brande, Denmark, Email: phicout@mek.dtu.dk
†Professor, Department of Mechanical Engineering.

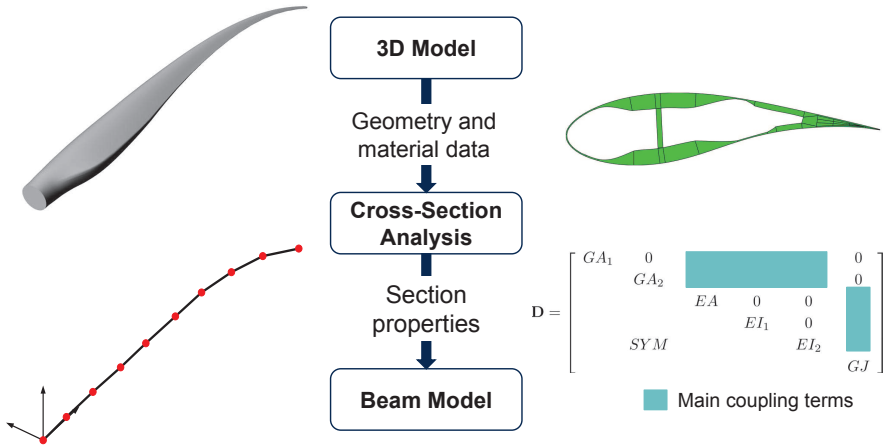

Figure 1: Structural blade modeling.

sections with coupling between the deformation modes has been developed. The stiffness matrix is evaluated using a single layer of 3D finite elements with cubic lengthwise displacement interpolation on which six independent deformation modes corresponding to extension, torsion, homogeneous bending and homogeneous shear are prescribed by imposing suitable displacement increments across the slice. The advantages of the present finite-thickness slice method are that it avoids the development of any special 2D theory for the stress and strain distributions over the cross-section and enables a simple and direct representation of material discontinuities and general anisotropy via their well established representation in 3D elements. The present cross-section analysis method has been implemented and validated in a computer program called CrossFlex (Cross-section Flexibility) for thin-walled and massive parts made of general anisotropic materials [1, 4, 5].

The accuracy of the six by six stiffness matrix as well as the ease to accommodate drastic geometry and material changes from previous designs using Finite Element based cross-section analysis methods largely depend on the discretization approach. The conventional finite element meshing approach is to model each layer in the blade walls using one or more elements through the thickness. Using this approach, the number of elements will depend on the number of layers which requires significant meshing effort and limits design flexibility. To circumvent these limitations, a new cross-section meshing approach was developed where thin to thick laminates are modelled using a single element through the wall thickness [2]. The elements stiffness is obtained from integration of the stiffness of the individual lamina across the thickness. A complementary postprocessing scheme was also developed to recover interlaminar stresses via equilibrium equations of 3D elasticity.

An illustrative comparison between the discretization of a lamina using conventional solid element and the internally layered elements is shown in Fig. 2. It can be seen that the conventional meshing approach requires several elements through the wall thickness whereas only one layered element is required to model the section of the lamina. Furthermore, by integrating the stiffness of the individual laminates the effect of the staking sequence is retained, e.g. stiff laminates closer to the outer surface of the blade shell should increase the bending stiffness. This information would be lost if the material properties of the element were taken as the thickness weighted average of the lamina properties. The reduced number of nodes and simpler mesh needed when using layered elements provide substantial pre-processing and computational effort savings compared with conventional meshing using solid elements. For example, less than 50 internally layered elements are needed to model the complexity of a typical blade cross-section [2].

The second step to create a reduced model of the 3D blade is to obtain the beam elements stiffness matrices. In the present project, a beam element was extended in which the stiffness properties are obtained via flexibility from equilibrium considerations that do not use assumed shape functions [3]. This so called complementary energy approach immediately accepts the six

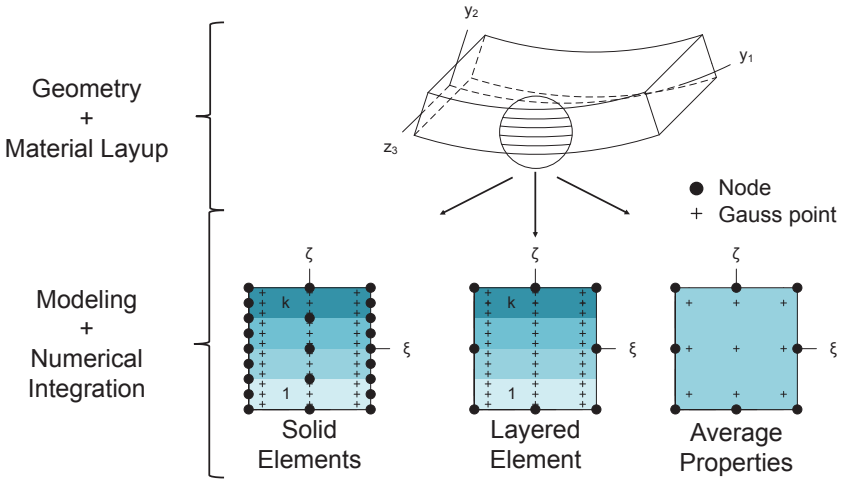

Figure 2: Comparison of laminate modeling methods.

by six cross-section stiffness matrices and accounts for geometry and material variations along the blade span. The beam element has been incorporated into an aeroelastic program at Siemens Wind Power A/S. It has been shown that a blade with complex geometry and material layup can accurately and effectively be modeled using 6-8 elements.

3 Applications

This section illustrates the application of the developed method of evaluating general cross-sectional properties and beam element stiffness matrices to model composite beams. Two studies are considered, first the cross-section properties and kinematics of a box beam with bend-twist coupling are studied and compared with published results. Second, the beam element capability is further demonstrated with its application to a realistic wind turbine rotor blade.

3.1 Box Beam

This example concerns the analysis of a composite box beam that exhibits bend-twist coupling via the use of off-axis fibers. The cross-section properties of this beam have been studied in Yu et al. [6] and by the present authors in Couturier and Krenk [4] to validate cross-sectional analysis theories. The box has a width of $w = 24.2\,\text{mm}$ (0.953 in.), a height of $h = 13.5\,\text{mm}$ (0.530 in.) and a uniform wall thickness of $t = 0.76\,\text{mm}$ (0.030 in.). The walls of the section are made up of six laminas with $E_i = 142.0\,\text{GPa}$ (20.59E+06 psi), $E_j = E_k = 9.79\,\text{GPa}$ (1.42E+06 psi), $G_{ij} = 6.00\,\text{GPa}$ (8.7E+05 psi), $G_{ik} = G_{jk} = 4.80\,\text{GPa}$ (6.96E+05 psi) and $\nu_{ij} = \nu_{ik} = \nu_{jk} = 0.42$ where i denotes the fiber direction, j the transverse direction, and k the direction normal to the plane of the lamina. The layup sequence for the top and bottom walls are $(-\alpha)_6$ and $(\alpha)_6$, respectively, and for left and right walls are $(-\alpha, \alpha)_3$ and $(\alpha, -\alpha)_3$, respectively. The layup sequence is defined from the innermost to the outermost layers.

In the current analysis, the cross-section is discretized using two meshes which are illustrated in Fig. 3. The first mesh, show in Fig. 3(a), represents the conventional highly discretized meshing approach with one element placed in each of the six layers in the thickness direction and 50 segments in the circumferential direction for a total of 300 solid elements. The elements have quadratic interpolation in the cross-section plane. The second mesh, show in Fig. 3(b), uses internally layered elements with a single element in the thickness direction. The walls are modelled using four 16-node elements with cubic-linear interpolation in the cross-section plane. Each corner is modelled using two triangular elements with linear interpolation in the cross-section plane. This discretization of the slice contains a total of 12 elements. Both meshes use lengthwise cubic Hermitian interpolation to capture the displacement field associated with prismatic beams. This results in the degrees of freedom to be concentrated on the front and back faces of the slice, as shown in Fig. 3. Note that a thickness of the slice comparable to the in-plane element dimensions

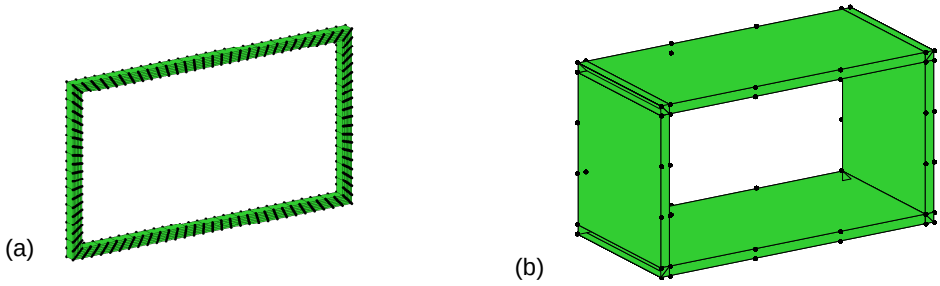

Figure 3: (a) Mesh using 300 solid elements, (b) Mesh using 12 solid internally layered elements.

is used to avoid ill-conditioned elements.

The particular cross-section with $\alpha = 15^\circ$ has been analysed using VABS with 300 6-noded quadralateral elements and NABSA with 336 9-noded quadralateral elements by Yu et al. [6]. These results are presented in Table 1 together with results obtained by the present method using the two meshes shown in Fig. 3. The $\alpha = 15^\circ$ configuration exhibits bend-twist coupling and extension-shear coupling. A measure of the importance of the off-diagonal terms in the cross-section stiffness matrix D can be obtained by normalizing them with respect to their associated diagonal terms,

$$\gamma_{ij} = \frac{D_{ij}}{\sqrt{D_{ii}\, D_{jj}}}. \tag{1}$$

This normalized measure of coupling, referred to as the coupling parameter, ranges from $-1 < \gamma_{ij} < 1$, where the extreme values indicate maximum possible coupling. All stiffness terms obtained using the present detailed mesh agree well with those calculated using VABS and NABSA. Good agreement is also obtained with the internally layered element model with one order of magnitude less elements with the maximum percentage difference when comparing the dominant terms of 1.5 $\%$ occurring for the shear stiffness in the x_2 direction. The bend-twist coupling parameter γ_{46} and the extension-shear coupling parameter γ_{13} have a 0.9 $\%$ and $0.5\,\%$ difference with the detailed models, respectively. It is noted that the differences on all parameters are smaller than the variability of the properties of fiber reinforced structures used in the industry.

Figure 4(a) shows the value of the bend-twist and extension-shear coupling parameter with respect to the ply angle obtained using the internally layered element model with 12 elements and the detailed mesh with 300 elements. It can be seen that both models agree well for all fiber orientations. The maximum bend-twist coupling occurs at a fiber orientation α =25° with a

Table 1: Cross-section stiffness properties for the box section with $\alpha = 15$.

	Units	NABSA 336 elements	VABS 300 elements	Present Full 300 elements	Present Lam. 12 elements
GA_1	[N]	3.94E+05	3.93E+05	3.94E+05	3.98E+05
GA_2	[N]	1.72E+05	1.73E+05	1.72E+05	1.75E+05
EA	[N]	6.09E+06	6.09E+06	6.08E+06	6.09E+06
EI_1	[Nm^2]	1.70E+02	1.70E+02	1.70E+02	1.70E+02
EI_2	[Nm^2]	4.05E+02	4.05E+02	4.06E+02	4.09E+02
GJ	[Nm^2]	4.88E+01	4.88E+01	4.87E+01	4.90E+01
γ_{12}		1.37E−03	1.23E−03	1.36E−03	1.38E−03
γ_{13}		−5.28E−01	−5.29E−01	−5.29E−01	−5.26E−01
γ_{23}		−6.51E−04	−5.67E−04	−6.33E−04	−1.60E−03
γ_{45}		−4.06E−03	−4.06E−03	−4.05E−03	−2.07E−03
γ_{46}		5.55E−01	5.55E−01	5.56E−01	5.52E−01
γ_{56}		−7.13E−03	−7.17E−03	−7.16E−03	−5.80E−03

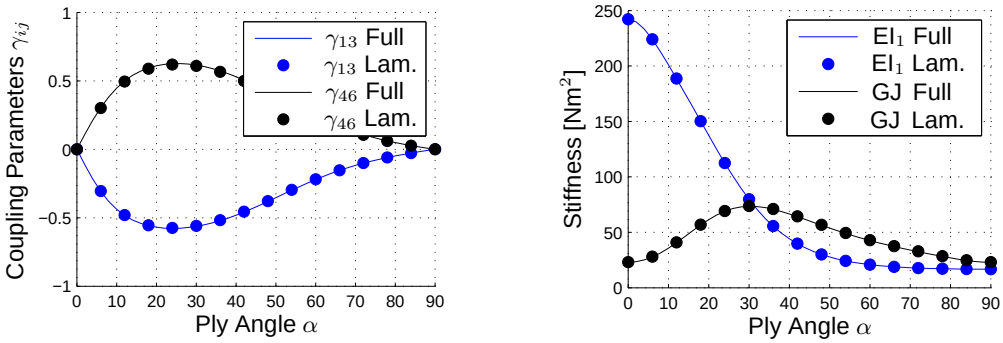

Figure 4: Stiffness properties as function of the fiber orientation angle α: (a) Bend-twist and extension-shear coupling coefficients, (b) Bending and torsion stiffnesses.

coupling value of γ_{46} =6.26E−01 while the maximum extension-shear coupling occurs at a fiber orientation α =24° with a coupling value of γ_{46} = −5.78E−01. The variation of the bending stiffness about the x_1 axis and the torsion stiffness with respect to the ply angle is shown in Fig. 4(b). It can be seen that using a fiber orientation $\alpha = 25°$ leads to a reduction of the bending stiffness of 56 % compared to the configuration with no off-axis fibers (i.e. 0°).

The linear static behaviour of a 762 mm (30 in.) long cantilever beam with such a section with a height of h =13.6 mm (0.537 in.) instead of h =13.5 mm (0.530 in.) built with three different fiber orientations $\alpha = 15°$, 30°, and 45° has been investigated experimentally by Chandra et al. [7]. The twist and bending slope at the middle of the beam they measured due to a tip torque are shown in Fig. 5 and Fig. 6, respectively, together with results obtain with the present modeling approach using a single beam element and the six by six stiffness matrix obtained using the two meshes shows in Fig. 3. Results are compared with data obtained from Smith and Chopra [8] using an analytical model (Smith and Chopra) and a finite element approach developed by Stample and Lee [9] (Stample and Lee), as well as data obtained from Ghiringhelli [10] using a finite element beam model (Ghiringhelli) and a 3D finite element model (3D FEM).

For the three beams modelled, the results obtained using the present beam model with the detailed cross-section mesh agree well with the 3D finite element model (3D FEM), the finite element beam model developed by Ghiringhelli (Ghiringhelli), as well as the beam model developed by Stample and Lee (Stample and Lee). Good agreement is also obtained with the experimental results with the exception of the bending slope for the beam with $\alpha = 30°$. Ghiringhelli [10] offers an explanation for this discrepancy. He shows by evaluating the bending slope at every 5° fiber angle interval that the experimental result at $\alpha = 30°$ deviates from the regular analytical curve.

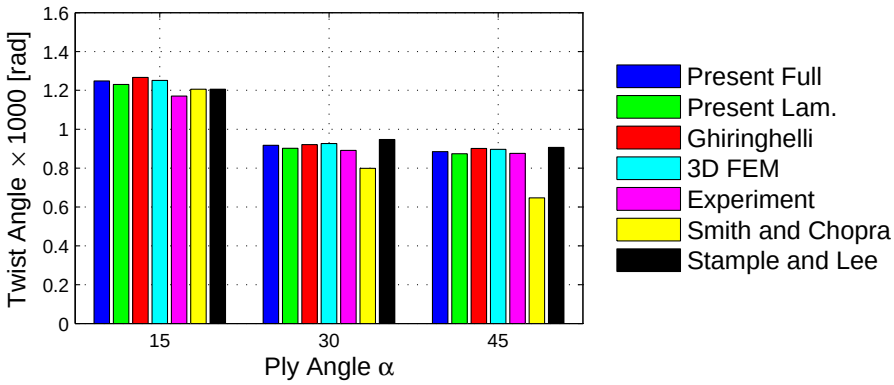

Figure 5: Twist at mid span of box beam under tip torque of 0.113 Nm [1 lb in.].

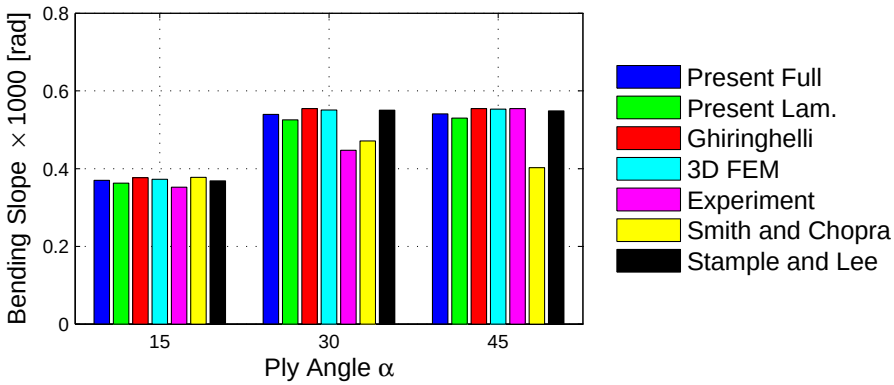

Figure 6: Bending slope at mid span of box beam under tip torque of 0.113 Nm [1 lb in.].

Very good agreement is also obtained when using the cross-section stiffness properties from the internally layered element model with the maximum percentage difference compared to using the stiffness properties of the detailed cross-section mesh of 2.6 % occurring for the bending slope with $\alpha = 30$.

3.2 Wind Turbine Blade

This second and final example of the present paper concerns the analysis of a 75 m long wind turbine blade manufactured by Siemens Wind Power A/S illustrated in Fig. 7. The blade is constructed using a single web design with the shell and spar cap made of fiberglass-epoxy, while the sandwich core present in the trailing edge walls and tail are made of balsa and foam. The distribution along the blade length of bending stiffnesses about the principal axes of bending normalized with respect to the bending stiffness of the circular root section are shown in Fig. 8. This gives an appreciation of the large cross-section property variations that must be captured when modeling wind turbine blades. It can be seen that the bending stiffness in the edgewise direction is on average for the first half of the blade twice as large as the stiffness in the flapwise direction. The increase in the edgewise bending stiffness near the root is associated with the transition from a circular to an airfoil cross-section.

In the current analysis, the blade is discretized using six beam element meshes each with a different number of elements. The location of the nodes for the different meshes used are shown in Fig. 7. The nodes are positioned along the neutral axis (elastic axis). Omitted from the figure for clarity are the mesh with 32 and 75 equally spaced elements. Note that the node positions for the mesh with four and eight elements are optimized to minimize the error of the first four natural frequencies. As expected, the nodes are skewed towards the more compliant outboard part of the blade, as shown in Fig. 7.

The relative error of the in-plane tip displacement obtained using the models with one, four, and sixteen elements relative to a reference deflection calculated using 75 elements under a concentrated tip load $p_1 = p_2 = c$ are shown in Fig. 9(a). Four elements are required to obtain convergence of both in-plane displacement components to within 1 % relative error. This is due

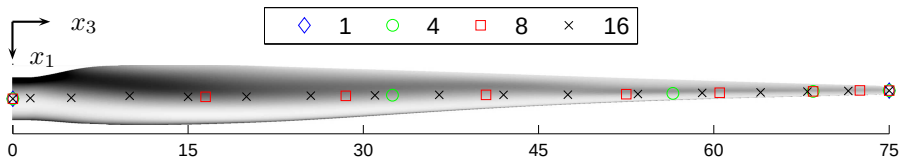

Figure 7: Rotor blade model discretization.

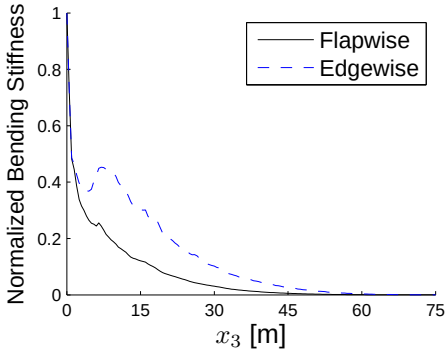

Figure 8: Normalized flapwise and edgewise bending stiffness.

to the inability of one element to capture the effect of the pre-bend in the blade. If the blade was straightened, the deflection under a tip load would be calculated exactly using a single element.

The relative error of the first four undamped natural frequencies of the blade obtained using the models with 4, 8, 16, and 32 elements relative to the frequencies calculated using 75 elements are shown in Fig. 9(b). The mass matrix is obtained from a finer integration of the classic shape functions. For this case, eight elements are required to obtained convergence of all four natural frequencies to within $1\,\%$ relative error. The increase in the number of elements required to describe the dynamic behaviour is expected from the large material property variations, where a sufficient number of elements is needed to properly capture the mode shapes associated with the natural frequencies.

4 Conclusion

A method of evaluating general cross-sectional properties and beam element stiffness matrices of a rotor blade which accounts for all the possible couplings between the deformation modes and of variations in geometry and material along the blade has been developed. The present methods avoid the need for advanced kinematic analysis of beams and instead hinge on the beam equilibrium modes.

In spite of the very small number of elements used, the method shows good agreement with numerical solutions and experimental data for a box beam that exhibits bend-twist coupling via the use of off-axis fibers. Example of an analysis of a Siemens rotor blade demonstrated that very few elements are needed to describe dynamic and static behaviour of blades using the proposed modeling approach.

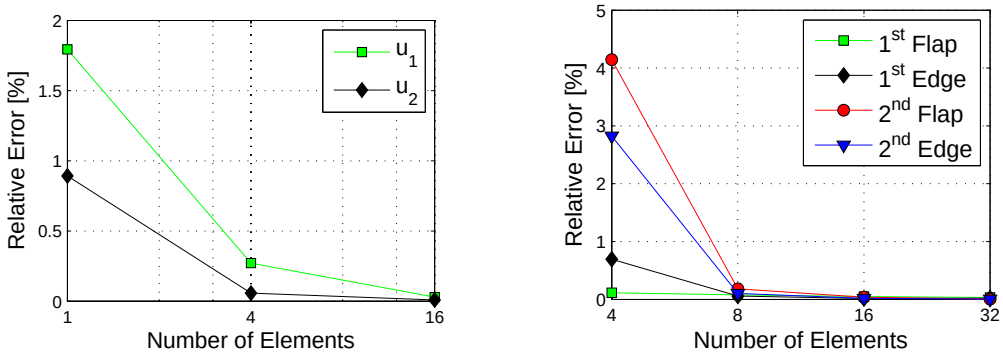

Figure 9: (a) Static tip deflection, (b) Undamped natural frequencies.

Acknowledgments
This work has been supported by Siemens Wind Power A/S.

References
[1] Couturier PJ, Krenk S, Høgsberg J. “Beam Section Stiffness Properties using a Single Layer of 3D Solid Elements.” *Computers and Structures*, 2015; 156:122–133.

[2] Couturier PJ, Krenk S. “Wind Turbine Cross-Sectional Stiffness Analysis using Internally Layered Solid Elements.” *AIAA Journal*, Submitted.

[3] Krenk S. “Element Stiffness Matrix for Beams with General Cross-Section Properties.” Report, Technical University of Denmark, Department of Mechanical Engineering, Denmark, 2006.

[4] Couturier P, Krenk S. “Composite Beam Cross-Section Analysis by a Single High-Order Element Layer.” *Proceedings of the 56th Structures, Structural Dynamics, and Materials Conference*, 2015; AIAA, Reston, Virginia, January.

[5] Couturier P, Krenk S. “General Beam Cross-Section Analysis using a 3D Finite Element Slice.” *Proceedings of the ASME 2014 International Mechanical Engineering Congress and Exposition*, 2014; ASME, November.

[6] Yu W, Hodges DH, Volovoi V, Cesnik CE. “On Timoshenko-Like Modeling of Initially Curved and Twisted Composite Beams.” *International Journal of Solids and Structures*, 2002; 39:5101–5121.

[7] Chandra R, Stemple AD, Chopra I. “Thin-Walled Composite Beams Under Bending, Torsional, and Extensional loads.” *Journal of Aircraft*, 1990; 27:619–626.

[8] Smith EC, Chopra I. “Formulation and Evaluation of an Analytical Model for Composite Box-Beams.” *J. Am. Helicopter Soc.*, 1991; 36:23–35.

[9] Stemple AD, Lee SW. “Finite-Element Model for Composite Beams with Arbitrary Cross-Sectional Warping.” *AIAA journal*, 1988; 26:1512–1520.

[10] Ghiringhelli GL. “On the Linear Three-Dimensional Behaviour of Composite Beams.” *Composites Part B: Engineering*, 1997; 28:613–626.